Eur. Phys. J. C 22, 283–287 (2001)
Digital Object Identifier (DOI) 10.1007/s100520100802

THE EUROPEAN PHYSICAL JOURNAL C

$\tau \to \omega 3\pi\nu$ decays

J. Gao, B.A. Li

Department of Physics and Astronomy, University of Kentucky, Lexington, KY 40506, USA

Received: 30 July 2001 /
Published online: 21 November 2001 –

Abstract. A theoretical study of the anomalous decay mode $\tau \to \omega\pi\pi\pi\nu$ is presented. The theoretical value of the branching ratio of $\tau^- \to \omega\pi^-\pi^0\pi^0\nu$ agrees well with the data. The branching ratio of $\tau^- \to \omega\pi^+\pi^-\pi^-\nu_\tau$ is predicted. It is found that the vertices of $a_1\rho\pi$ and $\omega\rho\pi$ play a dominant role in these two decay modes. CVC is satisfied, and there is no adjustable parameter.

There is rich physics in τ hadronic decays. Because of the value of m_τ many light mesons made of u, d, and s quarks, especially meson resonances, are produced in the decays. Therefore, τ mesonic decays provide a very unique test ground of the standard model and QCD. An effective QCD large N_C theory of mesons has been proposed to study the physics of light mesons [1]. In this theory the tree diagrams of mesons are at leading order of a large N_C expansion and loop diagrams are at higher orders. This theory has been applied to study many physical processes of mesons and it has been shown that the theory is phenomenologically successful [1–3]. Both vector and axial-vector currents contribute to τ decays. The mesonic vector current is obtained from the vector meson dominance (VMD) which is a natural result of this theory [1]. The axial-vector current of mesons is also obtained [3]. PCAC is satisfied [3]. Many τ mesonic decay modes have been studied by using this theory [3]. Theory agrees with the data reasonably well.

The decay rate of $\tau^- \to 2\pi^-\pi^+3\pi^0\nu_\tau$ has been measured by ALEPH [4] and CLEO [5] and predicted by CVC [6–8]. The first measurement of $\tau^- \to \omega\pi^-\pi^0\pi^0\nu_\tau$ has been reported by CLEO [5]:

$$B(\tau^- \to \omega\pi^-\pi^0\pi^0\nu_\tau) = (1.89^{+0.74}_{-0.67} \pm 0.40) \times 10^{-4}.$$

There is another decay mode: $\tau^- \to \omega\pi^+\pi^-\pi^-\nu_\tau$. These are very interesting decay modes resulting from the vector current. These decay modes are tests of VMD. The ω meson is associated with an anomaly. The Wess–Zumino–Witten anomaly [9] can be tested by these modes. Since four mesons are produced, many meson vertices are involved in these processes. These decay modes provide tests on all kinds of meson theory. In the effective theory of large N_C QCD of mesons [1] all the vertices of these decays have been derived and all the parameters have been fixed. The large N_C theory of mesons [1] will make definite predictions on these two decay modes. Therefore, they provide serious tests on this theory.

In this paper we apply the effective theory of large N_C QCD [1] to study $\tau^- \to \omega\pi^-\pi^0\pi^0\nu_\tau$ and $\tau^- \to \omega\pi^+\pi^-\pi^-\nu_\tau$. Only a vector current contributes to both decays, which has been derived [3] and was found to be

$$\mathcal{L}^V = \frac{g_W}{4}\cos\theta_C g \times \left\{-\frac{1}{2}(\partial_\mu A^i_\nu - \partial_\nu A^i_\mu)(\partial^\mu\rho^{i\nu} - \partial^\nu\rho^{i\mu}) + A^i_\mu j^{i\mu}\right\}, \quad (1)$$

where A^i_μ is the W boson field, and j^i_μ is derived by the substitution

$$\rho^i_\mu \to \frac{g_W}{4} g\cos\theta_C A^i_\mu \quad (2)$$

in the vertices involving the ρ meson and g is a universal coupling constant which is determined to be 0.39 by fitting $\rho \to ee^+$. Equation (1) is exactly the same expression of VMD as given by Sakurai [10].

The diagrams contributing to the decay $\tau \to \omega\pi\pi\pi\nu$ are shown in Figs. 1a–f. All the vertices are derived in the chiral limit. The $\omega\rho\pi$ vertex is the Wess–Zumino–Witten anomaly and is derived to be

$$\mathcal{L}^{\omega\rho\pi} = -\frac{3}{\pi^2 g^2 f_\pi}\varepsilon^{\mu\nu\alpha\beta}\partial_\mu\omega_\nu\rho^i_\alpha\partial_\beta\pi^i. \quad (3)$$

The vertex $\mathcal{L}^{\omega\rho\pi}$ leads to the Adler–Bell–Jackiw anomaly of $\pi^0 \to \gamma\gamma$ [1].

Besides the anomalous vertices $\mathcal{L}^{\omega\rho\pi}$, there are three other kinds of normal vertices in Fig. 1. The first kind of vertices derived in [1] are

$$\mathcal{L}^{a_1\rho\pi} = \epsilon_{ijk}\{A(q^2,p^2)a^i_\mu\rho^{j\mu}\pi^k - Ba^i_\mu\rho^j_\nu\partial^{\mu\nu}\pi^k + Da^i_\mu\partial^\mu(\rho^j_\nu\partial^\nu\pi^k)\}, \quad (4)$$

$$\mathcal{L}^{\rho\pi\pi} = \frac{2}{g}\epsilon_{ijk}\rho^i_\mu\pi^j\partial^\mu\pi^k - \frac{2}{\pi^2 f_\pi^2 g}\left\{\left(1-\frac{2c}{g}\right)^2 - 4\pi^2c^2\right\}\epsilon_{ijk}\rho^i_\mu\partial_\nu\pi^j\partial^{\mu\nu}\pi^k$$

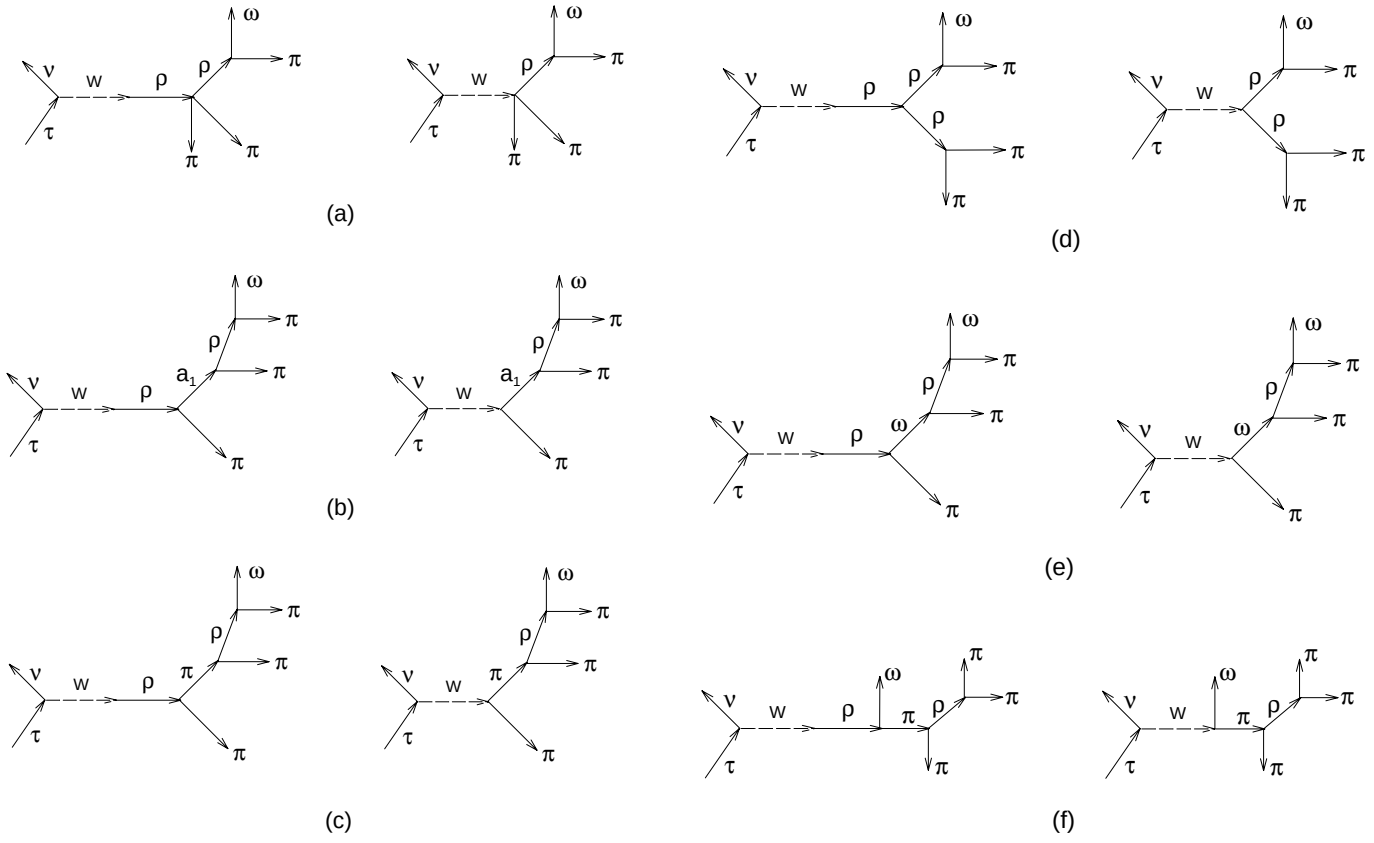

Fig. 1a–f. Feynman diagrams of $\tau \to \omega\pi\pi\pi\nu$

$$- \frac{1}{\pi^2 f_\pi^2 g}\left\{3\left(1-\frac{2c}{g}\right)^2 + 1 - \frac{2c}{g} - 8\pi^2 c^2\right\} \times \epsilon_{ijk}\rho_\mu^i \pi_j \partial^2 \partial_\mu \pi_k, \quad (5)$$

$$\mathcal{L}^{\rho\rho\rho} = -\frac{2}{g}\epsilon_{ijk}\partial_\mu \rho_\nu^i \rho^{j\mu}\rho^{k\nu}, \quad (6)$$

where

$$c = \frac{f_\pi^2}{2gm_\rho^2},$$

$$F^2 = \left(1-\frac{2c}{g}\right)^{-1} f_\pi^2,$$

$$A(q^2,p^2) = \frac{2}{f_\pi} f_a \left\{\frac{F^2}{g^2} + p^2\left[\frac{2c}{g} + \frac{3}{4\pi^2 g^2}\left(1-\frac{2c}{g}\right)\right] + q^2\left[\frac{1}{2\pi^2 g^2} - \frac{2c}{g} - \frac{3}{4\pi^2 g^2}\left(1-\frac{2c}{g}\right)\right]\right\}, \quad (7)$$

$$f_a = \left(1-\frac{1}{2\pi^2 g^2}\right)^{-1/2}, \quad (8)$$

$$B = -\frac{2}{f_\pi} f_a \frac{1}{2\pi^2 g^2}\left(1-\frac{2c}{g}\right), \quad (9)$$

$$D = -\frac{2}{f_\pi} f_a \left\{\frac{2c}{g} + \frac{3}{2\pi^2 g^2}\left(1-\frac{2c}{g}\right)\right\}, \quad (10)$$

q being the momentum of the a_1 meson and p the momentum of the ρ meson.

The vertices of $\mathcal{L}^{a_1\rho\pi}$ and $\mathcal{L}^{\rho\pi\pi}$ have been tested by the widths of a_1 and ρ, pion form factors, and other physical processes [1–3]. Theory agrees well with the data.

The second kind of normal vertices are contact interactions between two meson fields,

$$\mathcal{L}^{\pi\pi} = \frac{1}{4\pi^2 f_\pi^2}\left(1-\frac{2c}{g}\right)^2 \partial_{\mu\nu}\pi^i \partial^{\mu\nu}\pi^i, \quad (11)$$

$$\mathcal{L}^{\pi a} = \frac{f_a}{2\pi^2 g f_\pi}\left(1-\frac{2c}{g}\right)\partial_{\mu\nu}\pi^i \partial^\mu a^{i\nu}, \quad (12)$$

$$\mathcal{L}^{aa} = \frac{f_a^2}{4\pi^2 g^2}(\partial_\mu a^{i\mu})^2. \quad (13)$$

By inserting these vertices into Figs. 1b,c, related diagrams are obtained.

The third kind of vertex is the direct interaction between $\rho\rho\pi\pi$,

$$\mathcal{L}^{\pi\pi\rho\rho} = \frac{4}{f_\pi}\epsilon_{ijk}\epsilon_{ij'k'}\left\{\frac{F^2}{2g^2}\rho_\mu^j \rho_\mu^{j'}\pi_k\pi_{k'} + \left[-\frac{2c^2}{g^2} + \frac{3}{4\pi^2 g^2}\left(1-\frac{2c}{g}\right)^2\right]\rho_\mu^j \rho_\nu^{j'}\partial^\mu\pi_k\partial^\nu\pi_{k'}$$

$$
\begin{aligned}
&+\left[-\frac{2c^2}{g^2}+\frac{1}{4\pi^2 g^2}\left(1-\frac{2c}{g}\right)^2\right]\rho_\nu^i\rho^{j'\nu}\partial_\mu\pi_k\partial^\mu\pi_{k'}\\
&-\frac{2c^2}{g^2}\rho_\mu^j\rho_\nu^{k'}\partial^\nu\pi_k\partial^\mu\pi_{j'}\\
&-\frac{3}{2\pi^2 g^2}\left(1-\frac{2c}{g}\right)(\rho_\mu^j\pi_k\partial_\nu\pi_{j'}-\rho_\nu^j\pi_k\partial_\mu\pi_{j'})\partial^\nu\rho^{k'\mu}\\
&-\frac{1}{2\pi^2 g^2}\left(1-\frac{2c}{g}\right)\rho_\mu^j\pi_k\rho_\nu^{j'}\partial^{\mu\nu}\pi_{k'}\\
&+\frac{1}{4\pi^2 g^2}\left[\partial_\nu(\rho_\mu^j\pi_k)\partial^\nu(\rho_\mu^j\pi_{k'})\right.\\
&\left.+2\left(1-\frac{2c}{g}\right)\rho_\mu^j\pi_k\rho_\nu^{j'}\partial^{\mu\nu}\pi_{k'}\right]\Bigg\}. \qquad (14)
\end{aligned}
$$

This is the vertex of Fig. 1a.

Due to the structure of the vertex (1) the amplitudes of the diagrams Figs. 1e,f satisfy the CVC automatically. However, for the diagrams of Figs. 1a,b,c,d we have to put all the three kinds of vertices (4)–(6), (11)–(14) together to have CVC satisfied in the chiral limit. These vertices have been exploited to calculate the branching ratios of $\tau \to \rho\pi\pi\nu$ [11]. Theoretical results are in agreement with the data. It is necessary to emphasize that all the parameters of this study have been fixed in previous studies. There is no adjustable parameter in this investigation.

In the diagram of Fig. 1e there are two anomalous vertices $\mathcal{L}^{\omega\rho\pi}$. The study [1] shows that the strength of this vertex is weaker than normal vertices. This is the reason why the ω meson has a narrower decay width than the ρ meson. The calculation shows that the contribution of the diagram of Fig. 1e is negligible. In Fig. 1f there are a ρ resonance and ω and π mesons in the final state. Because the phase space of this process is too small, the contribution of this diagram is also negligible.

Now we calculate the branching ratios of $\tau \to \omega\pi\pi\pi\nu$. This is very lengthy. The amplitudes of the decays $\tau \to \omega\pi\pi\pi\nu$ are obtained from all the three kinds of vertices (4)–(6), (11)–(14) and the vertex $\mathcal{L}^{\omega\rho\pi}$ of (3). In the chiral limit the matrix elements of the vector current of $\tau^- \to \omega\pi^-\pi^0\pi^0\nu_\tau$ and $\tau^- \to \omega\pi^+\pi^-\pi^-\nu_\tau$ have been found to be

$$
\begin{aligned}
&\langle\omega(p)\pi^0(p_1)\pi^0(p_2)\pi^-(p_3)\mid j^{\mu-}\mid 0\rangle\\
&=\frac{1}{\sqrt{16E\omega_1\omega_2\omega_3}}\left(g^{\mu\lambda}-\frac{q^\mu q^\lambda}{q^2}\right)\frac{3}{\pi^2 g f_\pi}\\
&\times\frac{-m_\rho^2+\mathrm{i}\sqrt{q^2}\Gamma_\rho(q^2)}{q^2-m_\rho^2+\mathrm{i}\sqrt{q^2}\Gamma_\rho(q^2)}f_\lambda^{00}, \qquad (15)\\
&f_\lambda^{00}=\epsilon_{\nu'}p_{\mu'}\varepsilon^{\mu'\nu'\alpha\beta}\\
&\times\left\{\frac{p_{3\beta}}{(p+p_3)^2-m_\rho^2+\mathrm{i}\sqrt{(p+p_3)^2}\Gamma_\rho((p+p_3)^2)}\right.\\
&\times(f_{\alpha\lambda}^{(12)}(p+p_3)+f_{\alpha\lambda}^{(21)}(p+p_3))\\
&-\frac{p_{1\beta}}{(p+p_1)^2-m_\rho^2+\mathrm{i}\sqrt{(p+p_1)^2}\Gamma_\rho((p+p_1)^2)}\\
&\times f_{\alpha\lambda}^{(23)}(p+p_1)\\
&-\frac{p_{2\beta}}{(p+p_2)^2-m_\rho^2+\mathrm{i}\sqrt{(p+p_2)^2}\Gamma_\rho((p+p_2)^2)}\\
&\left.\times f_{\alpha\lambda}^{(13)}(p+p_2)\right\}, \qquad (16)\\
&\langle\omega(p)\pi^+(p_2)\pi^-(p_1)\pi^-(p_3)\mid j^{\mu-}\mid 0\rangle\\
&=\frac{1}{\sqrt{16E\omega_1\omega_2\omega_3}}\left(g^{\mu\lambda}-\frac{q^\mu q^\lambda}{q^2}\right)\\
&\times\frac{3}{\pi^2 g f_\pi}\frac{-m_\rho^2+\mathrm{i}\sqrt{q^2}\Gamma_\rho(q^2)}{q^2-m_\rho^2+\mathrm{i}\sqrt{q^2}\Gamma_\rho(q^2)}f_\lambda^{--}, \qquad (17)\\
&f_\lambda^{--}=\epsilon_{\nu'}p_{\mu'}\varepsilon^{\mu'\nu'\alpha\beta}\\
&\times\left\{\frac{p_{3\beta}}{(p+p_3)^2-m_\rho^2+\mathrm{i}\sqrt{(p+p_3)^2}\Gamma_\rho((p+p_3)^2)}\right.\\
&\times f_{\alpha\lambda}^{(12)}(p+p_3)\\
&+\frac{p_{1\beta}}{(p+p_1)^2-m_\rho^2+\mathrm{i}\sqrt{(p+p_1)^2}\Gamma_\rho((p+p_1)^2)}\\
&\times f_{\alpha\lambda}^{(32)}(p+p_1)\\
&-\frac{p_{2\beta}}{(p+p_2)^2-m_\rho^2+\mathrm{i}\sqrt{(p+p_2)^2}\Gamma_\rho((p+p_2)^2)}\\
&\left.\times(f_{\alpha\lambda}^{(13)}(p+p_2)+f_{\alpha\lambda}^{(31)}(p+p_2))\right\}, \qquad (18)
\end{aligned}
$$

where

$$
q=p+p_1+p_2+p_3, \qquad (19)
$$

$$
\begin{aligned}
f_{\alpha\lambda}^{(12)}(p_\rho)&=g_{\alpha\lambda}f(p_\rho)+p_{1\alpha}[f_{11}(p_\rho)p_{1\lambda}+f_{21}(p_\rho)p_{2\lambda}]\\
&+p_{2\alpha}[f_{12}(p_\rho)p_{1\lambda}+f_{22}(p_\rho)p_{2\lambda}], \qquad (20)
\end{aligned}
$$

with p_ρ being the momentum of the ρ meson, p_i ($i=1,2,3$) the momentum of pion, and p the momentum of ω. $f_{\alpha\lambda}^{(21)}$ is obtained from $f_{\alpha\lambda}^{(12)}$ by exchanging $p_1 \leftrightarrow p_2$; $f_{\alpha\lambda}^{(23)}$ is obtained from $f_{\alpha\lambda}^{(21)}$ by replacing p_1 with p_3; $f_{\alpha\lambda}^{(13)}$ is obtained from $f_{\alpha\lambda}^{(12)}$ by replacing p_2 with p_3; $f_{\alpha\lambda}^{(32)}$ is obtained from $f_{\alpha\lambda}^{(23)}$ by exchanging $p_2 \leftrightarrow p_3$; $f_{\alpha\lambda}^{(31)}$ is obtained from $f_{\alpha\lambda}^{(13)}$ by exchanging $p_1 \leftrightarrow p_3$. Γ_ρ is the decay width of the ρ meson of momentum q,

$$
\begin{aligned}
\Gamma_\rho(q^2)&=\frac{\sqrt{q^2}}{12\pi g^2}\left\{1+\frac{q^2}{2\pi^2 f_\pi^2}\left[\left(1-\frac{2c}{g}\right)^2-4\pi^2c^2\right]\right\}^2\\
&\times\left(1-\frac{4m_\pi^2}{q^2}\right)^{3/2}. \qquad (21)
\end{aligned}
$$

Equations (15) and (17) show that the CVC, indeed, is satisfied in the chiral limit. It is interesting to notice that the resonance factor

$$
\frac{-m_\rho^2+\mathrm{i}\sqrt{q^2}\Gamma_\rho(q^2)}{q^2-m_\rho^2+\mathrm{i}\sqrt{q^2}\Gamma_\rho(q^2)}
$$

in (15) and (17) is obtained from the combination of the two terms in (1). These two terms are shown in the two diagrams of Figs. 1a–f.

The contributions of the a_1 meson (Fig. 1b) to the functions f and f_{ij} $(i,j=1,2)$ are given below. The contributions from other diagrams are shown in the appendix. We have

$$\begin{aligned}
BW(k_1^2) &= \frac{1}{k_1^2 - m_a^2 + \mathrm{i}\sqrt{k_1^2}\Gamma_a(k_1^2)},\\
f(p_\rho) &= BW(k_1^2)A(q^2,k_1^2)A(p_\rho^2,k_1^2),\\
f_{11}(p_\rho) &= BW(k_1^2)A(p_\rho^2,k_1^2)B,\\
f_{12}(p_\rho) &= BW(k_1^2)\{[A(p_\rho^2,k_1^2)+A(q^2,k_1^2)]D\\
&\quad + (k_1\cdot p_2 - k_1\cdot p_1)BD + p_1\cdot p_2 B^2 - k_1^2 D^2\}\\
&\quad - BW(k_1^2)\frac{1}{m_a^2}\{-A(q^2,k_1^2) + k_1\cdot p_1 B + k_1^2 D\}\\
&\quad \times \{A(p_\rho^2,k_1^2) + k_1\cdot p_2 B - k_1^2 D\},\\
f_{22}(p_\rho) &= BW(k_1^2)A(q^2,k_1^2)B, \qquad (22)
\end{aligned}$$

where $k_i = q - p_i$ $(i=1,2,3)$ and

$$m_a^2 = \left(\frac{F^2}{g^2} + m_\rho^2\right) \Big/ \left(1 - \frac{1}{2\pi^2 g^2}\right). \qquad (23)$$

The decay width of a_1 meson is derived as

$$\begin{aligned}
\Gamma_a(k^2) &= \frac{k_a}{12\pi}\frac{1}{k^2}\left\{\left(3 + \frac{k_a^2}{m_\rho^2}\right)A^2(m_\rho^2,k^2)\right.\\
&\quad \left. - A(m_\rho^2,k^2)B(k^2+m_\rho^2)\frac{k_a^2}{m_\rho^2} + \frac{k^2}{m_\rho^2}k_a^4 B^2\right\},\\
k_a^2 &= \frac{1}{4k^2}(k^2 + m_\rho^2 - m_\pi^2)^2 - m_\rho^2. \qquad (24)
\end{aligned}$$

The decay rate of $\tau \to \omega\pi\pi\pi\nu$ is derived from (15)–(18)

$$\begin{aligned}
\frac{\mathrm{d}\Gamma^{ab}}{\mathrm{d}q^2} &= \frac{1}{128}\frac{G^2}{(2\pi)^8}\cos^2\theta_{\mathrm{C}}\frac{1}{q^2}\frac{1}{m_\tau^3}(m_\tau^2 - q^2)^2(m_\tau^2 + 2q^2)\\
&\quad \times \left(\frac{3}{\pi^2 g f_\pi}\right)^2 \frac{m_\rho^4 + q^2\Gamma_\rho^2(q^2)}{(q^2 - m_\rho^2)^2 + q^2\Gamma_\rho^2(q^2)}F^{ab}(q^2), \qquad (25)
\end{aligned}$$

where

$$\begin{aligned}
ab &= 00 \ \text{ or } \ --,\\
F^{ab}(q^2) &= \frac{1}{3}\left(g^{\lambda\lambda'} - \frac{q^\lambda q^{\lambda'}}{q^2}\right)\frac{1}{4(2\pi)^2}\\
&\quad \times \int \frac{\mathrm{d}^3p_1\mathrm{d}^3p_2\mathrm{d}^3p_3\mathrm{d}^3p}{E\omega_1\omega_2\omega_3}\delta(q - p_1 - p_2 - p_3 - p)\\
&\quad \times f_\lambda^{ab} f_{\lambda'}^{*ab}. \qquad (26)
\end{aligned}$$

The branching ratios of the two decay channels are calculated to be

$$B(\tau^- \to \omega\pi^-\pi^0\pi^0\nu_\tau) = 2.16\times 10^{-4}, \qquad (27)$$
$$B(\tau^- \to \omega\pi^+\pi^-\pi^-\nu_\tau) = 2.18\times 10^{-4}. \qquad (28)$$

The theoretical branching ratio of $\tau^- \to \omega\pi^-\pi^0\pi^0\nu_\tau$ is consistent with the data [5]. The theory predicts that the branching ratio of $\tau^- \to \omega\pi^+\pi^-\pi^-\nu_\tau$ is about the same as that of $\tau^- \to \omega\pi^-\pi^0\pi^0\nu_\tau$.

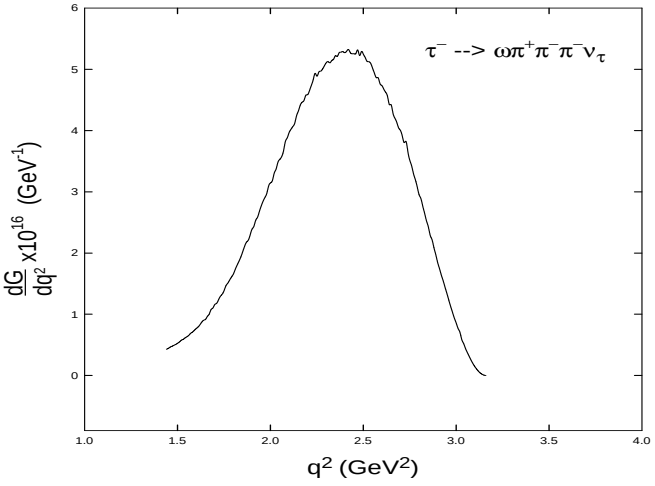

Fig. 2. Distribution function $\mathrm{d}\Gamma/\mathrm{d}q^2$ for $\tau^- \to \omega\pi^+\pi^-\pi^-\nu_\tau$

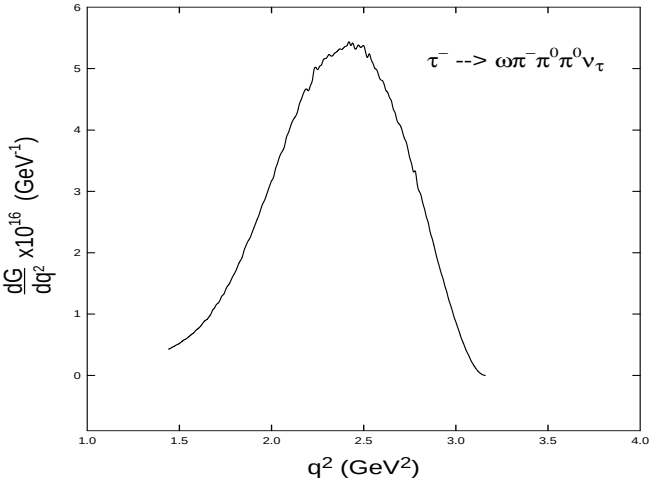

Fig. 3. Distribution function $\mathrm{d}\Gamma/\mathrm{d}q^2$ for $\tau^- \to \omega\pi^-\pi^0\pi^0\nu_\tau$

As shown in Fig. 1, there are many subprocesses in the decays. However, the calculation shows that the a_1 meson (Fig. 1b) dominates the two decay channels. If only the subprocess which is obtained from $\mathcal{L}^{a_1\rho\pi}$ is kept in the matrix elements (15) and (17), we obtain

$$B(\tau^- \to \omega\pi^-\pi^0\pi^0\nu_\tau) = 1.86\times 10^{-4}, \qquad (29)$$
$$B(\tau^- \to \omega\pi^-\pi^-\pi^+\nu_\tau) = 1.87\times 10^{-4}. \qquad (30)$$

86% of the decay rate comes from $\mathcal{L}^{a_1\rho\pi}$. It is necessary to point out that in Fig. 1b there are terms which violate CVC. However, these terms are cancelled by the corresponding terms of other diagrams. The results (29) and (30) are obtained after this cancellation. It is interesting to notice that the a_1 meson is associated with the a_1 dominance in the axial-vector current [3].

The distribution functions of the two decay modes, $\mathrm{d}\Gamma/\mathrm{d}q^2$, are calculated and shown in Figs. 2 and 3. There

is a peak in each distribution, which originates in the combination of the a_1 resonance and the kinematics of the decays.

To conclude, two decay modes of $\tau \to \omega\pi\pi\pi\nu$ have been studied by an effective large N_C application of QCD to the mesons. CVC is satisfied in the chiral limit. The theoretical branching ratio of $\tau^- \to \omega\pi^-\pi^0\pi^0\nu_\tau$ agrees with the data. The theory predicts that the branching ratio of $\tau^- \to \omega\pi^+\pi^-\pi^-\nu_\tau$ is about the same as that of $\tau^- \to \pi^-\pi^0\pi^0\nu_\tau$. In this study there is no adjustable parameter.

Acknowledgements. The authors wish to thank M. Barnett. This study is supported by DOE grant No. DE-91ER75661.

Appendix

(1) Diagrams involving the vertices (11)–(13).

$$\begin{aligned} f_{12}(p_\rho) = {} & \frac{1}{2\pi^2 g^2} f_a^2 \frac{1}{m_a^4}\{-A(q^2,k_1^2) + k_1\cdot p_1 B + k_1^2 D\} \\ & \times\{A(p_\rho^2,k_1^2) + k_1\cdot p_2 B - k_1^2 D\} \\ & + \frac{1}{2\pi^2 g f_\pi} f_a \frac{1}{m_a^2}\left(1-\frac{2c}{g}\right) \\ & \times\{-A(q^2,k_1^2) + k_1\cdot p_1 B + k_1^2 D\} \\ & \times\{2F_1(-k_1\cdot p_2) - k_1^2 F_2\} \\ & - \frac{1}{2\pi^2 g f_\pi} f_a \left(1-\frac{2c}{g}\right)\frac{1}{m_a^2} \\ & \times\{A(p_\rho^2,k_1^2) + k_1\cdot p_2 B - k_1^2 D\} \\ & \times\{2F_1(k_1\cdot p_1) - k_1^2 F_2\} \\ & - \frac{1}{2\pi^2 f_\pi^2}\left(1-\frac{2c}{g}\right)^2 \{2F_1(k_1\cdot p_1) - k_1^2 F_2\} \\ & \times\{2F_1(-k_1\cdot p_2) - k_1^2 F_2\}, \end{aligned} \tag{31}$$

where

$$F_1(q_1\cdot q_2) = \frac{2}{g}\left\{1 + \frac{1}{\pi^2 f_\pi^2} q_1\cdot q_2 \left[\left(1-\frac{2c}{g}\right)^2 - 4\pi^2 c^2\right]\right\}, \tag{32}$$

$$F_2 = \frac{4}{f_\pi^2}\left[\frac{2c^2}{g} - \frac{3}{4\pi^2 g}\left(1-\frac{2c}{g}\right)^2 - \frac{1}{4\pi^2 g}\left(1-\frac{2c}{g}\right)\right]. \tag{33}$$

(2) Diagrams of Fig. 1c.

$$\begin{aligned} f_{12}(p_\rho) = {} & -\frac{1}{k_1^2}\Big\{ -4F_1(k_1\cdot p_1)F_1(-k_1\cdot p_2) \\ & + 2k_1^2 F_2 F_1(-k_1\cdot p_2) \\ & + 2k_1^2 F_2 F_1(k_1\cdot p_1) - k_1^4 F_2^2\Big\}. \end{aligned} \tag{34}$$

(3) Diagrams of Fig. 1a.

$$\begin{aligned} f(p_\rho) = {} & \frac{4}{f_\pi^2}\left\{\frac{F^2}{g^2} - 2p_1\cdot p_2\left[-\frac{2c^2}{g^2} + \frac{1}{4\pi^2 g^2}\left(1-\frac{2c}{g}\right)^2\right]\right. \\ & \left. - \frac{3}{2\pi^2 g^2}\left(1-\frac{2c}{g}\right)(p_2\cdot p_\rho - q\cdot p_1) + \frac{k_1^2}{2\pi^2 g^2}\right\}, \\ f_{11}(p_\rho) = {} & -\frac{2}{\pi^2 g^2 f_\pi^2}\left(1-\frac{2c}{g}\right), \\ f_{12}(p_\rho) = {} & -\frac{8}{f_\pi^2}\left\{-\frac{2c^2}{g^2} + \frac{3}{4\pi^2 g^2}\left(1-\frac{2c}{g}\right)^2\right. \\ & \left. + \frac{3}{2\pi^2 g^2}\left(1-\frac{2c}{g}\right)\right\}, \\ f_{21}(p_\rho) = {} & \frac{8}{f_\pi^2}\left\{-\frac{4c^2}{g^2} + \frac{3}{4\pi^2 g^2}\left(1-\frac{2c}{g}\right)\right\}, \\ f_{22}(p_\rho) = {} & f_{11}(p_\rho). \end{aligned} \tag{35}$$

(4) Diagrams of Fig. 1d.

$$\begin{aligned} BW = {} & \frac{1}{(p_1+p_2)^2 - m_\rho^2 + \mathrm{i}\sqrt{(p_1+p_2)^2}\Gamma_\rho((p_1+p_2)^2)}, \\ f(p_\rho) = {} & \frac{8}{g^2} BW\, q\cdot(p_2-p_1) \\ & \times\left\{1 + \frac{p_1\cdot p_2}{\pi^2 f_\pi^2}\left[\left(1-\frac{2c}{g}\right)^2 - 4\pi^2 c^2\right]\right\}, \\ f_{12}(p_\rho) = {} & \frac{16}{g^2} BW\left\{1 + \frac{p_1\cdot p_2}{\pi^2 f_\pi^2}\left[\left(1-\frac{2c}{g}\right)^2 - 4\pi^2 c^2\right]\right\}, \\ f_{21}(p_\rho) = {} & -f_{12}(p_\rho). \end{aligned} \tag{36}$$

References

1. B.A. Li, Phys. Rev. D **52**, 5165, 5184 (1995)
2. D.N. Gao, B.A. Li, M.L. Yan, Phys. Rev. D **56**, 4115 (1997); B.A. Li, D.N. Gao, M.L. Yan, Phys. Rev. D **58**, 094031 (1998); J. Gao, B.A. Li, Phys. Rev. D **61**, 113006 (2000)
3. B.A. Li, Phys. Rev. D **55**, 1436, 1425 (1997); Phys. Rev. D **57**, 1790 (1998)
4. D. Buskulic et al., ALEPH Collaboration, Z. Phys. C **70**, 579 (1996)
5. S. Anderson, Phys. Rev. Lett. **79**, 3814 (1997)
6. R.J. Bobie, Z. Phys. C **69**, 99 (1995)
7. A. Rouge, Z. Phys. C **70**, 65 (1996)
8. S.I. Eidelman, V.N. Ivanchenko, Nucl. Phys. C (Proc. Suppl.) **55**, 181 (1997)
9. J. Wess, B. Zumino, Phys. Lett. B **37**, 95 (1971); E. Witten, Nucl. Phys. B **223**, 422 (1983)
10. J.J. Sakurai, Currents and mesons (University of Chicago Press 1969)
11. Bing An Li, Phys. Rev. D **58**, 097302 (1998)